Acta Crystallographica Section D
Biological Crystallography
ISSN 0907-4449

Covalent modifications of the catalytic tyrosine in octahaem cytochrome *c* nitrite reductase and their effect on the enzyme activity

Anton A. Trofimov,[a,b]* Konstantin M. Polyakov,[a,c] Tamara V. Tikhonova,[b] Alexey V. Tikhonov,[b] Tatyana N. Safonova,[b] Konstantin M. Boyko,[b,c] Pavel V. Dorovatovskii[c] and Vladimir O. Popov[b,c]

[a]Engelhardt Institute of Molecular Biology, Russian Academy of Sciences, ul. Vavilova 32, Moscow 119991, Russian Federation, [b]Bach Institute of Biochemistry, Russian Academy of Sciences, Leninskii pr. 33, Moscow 119071, Russian Federation, and [c]Russian Research Center 'Kurchatov Institute', Academic Kurchatov sq. 1, Moscow 123182, Russian Federation

Correspondence e-mail: burayatina@gmail.com

Received 1 September 2011
Accepted 6 December 2011

PDB References: TvNiR–NO_2, 3rkh; TvNiRb–PO_4, 3sce; TvNiRb–SO_3, 3lgq; TvNiRb–SO_3(MV), 3lg1; TvNiRb–NH_2OH, 3s7w; TvNiRb–H_2O, 3uu9.

Octahaem cytochrome *c* nitrite reductase from *Thioalkalivibrio nitratireducens* (TvNiR), like the previously characterized pentahaem nitrite reductases (NrfAs), catalyzes the six-electron reductions of nitrite to ammonia and of sulfite to sulfide. The active site of both TvNiR and NrfAs is formed by the lysine-coordinated haem and His, Tyr and Arg residues. The distinguishing structural feature of TvNiR is the presence of a covalent bond between the CE2 atom of the catalytic Tyr303 and the S atom of Cys305, which might be responsible for the higher nitrite reductase activity of TvNiR compared with NrfAs. In the present study, a new modified form of the enzyme (TvNiRb) that contains an additional covalent bond between Tyr303 CE1 and Gln360 CG is reported. Structures of TvNiRb in complexes with phosphate (1.45 Å resolution) and sulfite (1.8 Å resolution), the structure of TvNiR in a complex with nitrite (1.83 Å resolution) and several additional structures were determined. The formation of the second covalent bond by Tyr303 leads to a decrease in both the nitrite and sulfite reductase activities of the enzyme. Tyr303 is located at the exit from the putative proton-transport channel to the active site, which is absent in NrfAs. This is an additional argument in favour of the involvement of Tyr303 as a proton donor in catalysis. The changes in the activity of cytochrome *c* nitrite reductases owing to the formation of Tyr–Cys and Tyr–Gln bonds may be associated with changes in the pK_a value of the catalytic tyrosine.

1. Introduction

Bacterial pentahaem cytochrome *c* nitrite reductases (NrfAs) are key enzymes involved in dissimilatory nitrite reduction in the bacterial nitrogen cycle (Richardson & Watmough, 1999; Simon, 2002; Kern & Simon, 2009). They catalyze the six-electron reductions of nitrite to ammonia and of sulfite to sulfide and the two-electron reduction of hydroxylamine to ammonia. The nitrite reductase activity is two to three orders higher than the sulfite reductase activity. All NrfAs structurally characterized to date (Einsle *et al.*, 1999, 2000; Bamford *et al.*, 2002; Cunha *et al.*, 2003; Rodrigues *et al.*, 2006) are homodimers, with each subunit folded as a single domain containing five haems *c*. The haem arrangement is conserved in all NrfAs. Four of these haems have a standard bis-histidine coordination, whereas the active-site haem is coordinated by lysine on the proximal side and by water/hydroxyl on the distal side. The active site of NrfAs comprises conserved histidine, tyrosine and arginine residues. NrfAs bind up to two calcium ions, one of which is located close to the enzyme active site and is supposed to contribute to its proper structural organ-

Table 1
Conditions for the preparation of TvNiR and TvNiRb complexes by cocrystallization.

Complex	Protein solution	Reservoir solution
TvNiR–NO_2	11.6 mg ml^{-1} TvNiR, 0.02 *M* sodium tetraborate, 0.05 *M* Tris–HCl pH 8.0	0.2 *M* ammonium acetate, 0.1 *M* trisodium citrate pH 5.6, 30% 2-methyl-2,4-pentanediol, 0.1 *M* sodium nitrite
TvNiRb–H_2O		0.2 *M* trisodium citrate, 0.1 *M* Tris–HCl pH 8.5, 30%(*v*/*v*) PEG 400, 0.1 *M* hydroxylamine
TvNiRb–PO_4	9.3 mg ml^{-1} TvNiRb, 0.1 *M* potassium phosphate buffer pH 7.0	0.2 *M* trisodium citrate, 0.1 *M* Tris–HCl pH 8.5, 30%(*v*/*v*) PEG 400
TvNiRb–SO_3(MV)	Obtained by soaking a crystal of TvNiRb–PO_4 in a reservoir solution containing 0.08 *M* Na_2SO_3, 0.13 *M* $NaBH_4$ and 0.02 *M* methyl viologen (MV) for 10 min	
TvNiRb–SO_3	10.0 mg ml^{-1} TvNiRb, 0.05 *M* Tris–HCl pH 7.2	0.2 *M* ammonium acetate, 0.1 *M* trisodium citrate pH 5.6, 30% 2-methyl-2,4-pentanediol, 0.1 *M* sodium sulfite
TvNiRb–NH_2OH		0.09 *M* HEPES–NaOH pH 7.5, 1.26 *M* trisodium citrate, 10%(*v*/*v*) glycerol, 0.1 *M* hydroxylamine

ization. The proposed mechanism of nitrite reduction by NrfAs involves alternate electron and proton transfer to the substrate and reaction intermediates bound to the haem iron ion (Einsle *et al.*, 2002). The structure of a mutant form of NrfA in which the catalytic tyrosine residue was replaced by phenylalanine has been determined by Lukat *et al.* (2008). The nitrite reductase activity of the mutant form was 0.7% of that of the wild-type enzyme. The sulfite reductase activity remained unchanged.

The octahaem cytochrome *c* nitrite reductase TvNiR was isolated from the haloalkaliphilic sulfur-oxidizing γ-proteobacterium *Thioalkalivibrio nitratireducens* (Sorokin *et al.*, 2003). The enzyme functions as a hexamer with a molecular weight of 384 kDa. Like NrfA, it catalyzes the reductions of nitrite and hydroxylamine to ammonia and of sulfite to sulfide (Tikhonova *et al.*, 2006). The nitrite reductase activity of TvNiR is higher than that of NrfAs (Tikhonova *et al.*, 2006), whereas the sulfite reductase activity is lower (Trofimov, Polyakov, Boyko, Tikhonova *et al.*, 2010). The latter is similar to the activities of sirohaem-containing sulfite reductases. However, taking into account the fact that the sulfite reductase activity of TvNiR is absent at physiological pH values ($\sim$9.5), it is likely that TvNiR has a different function in cells.

Structures of the free form of TvNiR (Polyakov *et al.*, 2009) and TvNiR in complexes with the substrates nitrite (Polyakov *et al.*, 2009) and sulfite (Trofimov, Polyakov, Boyko, Tikhonova *et al.*, 2010) and the inhibitors azide (Polyakov *et al.*, 2009), cyanide (Trofimov, Polyakov, Boyko, Tikhonova *et al.*, 2010), and phosphate (Trofimov, Polyakov, Boyko, Filimonenkov *et al.*, 2010) have been determined previously. The TvNiR subunit consists of two domains: the N-terminal domain, which has a unique protein fold, and the catalytic domain, which is similar to the NrfA subunit. The N-terminal domain accommodates the first three haems. The catalytic domain houses the remaining five haems, which are arranged in the same fashion as in NrfA. The active site in TvNiR, like that in NrfA, is formed by the lysine-coordinated (Lys188) haem (haem 4) and histidine, tyrosine and arginine residues (His361, Tyr303 and Arg131). A calcium ion is located near the active site of TvNiR and is coordinated by conserved residues in TvNiR and NrfAs (Glu302, Tyr303, Lys358 and Gln360). In contrast to NrfA, the CE2 atom of the catalytic Tyr303 residue in TvNiR is covalently bound to the S atom of Cys305. The formation of a Tyr–Cys bond in the active site of TvNiR leads to a decrease in the pK_a value of the tyrosine hydroxyl [by 0.5 units for *o*-(methylthio)phenol; Himo *et al.*, 2002] and a more compact and rigid structure of the active site compared with the active site where this bond is absent (in NrfAs). These changes may be responsible for the higher catalytic activity of TvNiR in nitrite reduction compared with NrfAs (Polyakov *et al.*, 2009).

Previously, a bond between the CE atom of tyrosine and the S atom of cysteine has been found in the structures of galactose oxidase (Ito *et al.*, 1991), of eukaryotic cysteine dioxygenases (Joseph & Maroney, 2007) and of sirohaem-containing nitrite reductase from *Mycobacterium tuberculosis* (Schnell *et al.*, 2005). The covalently bound tyrosine and cysteine are located in the active sites of these enzymes and are important for their function. In the case of galactose oxidase, formation of the Tyr radical is necessary for substrate oxidation. This radical is stabilized both by the Tyr–Cys bond itself and by the stacking with a Trp residue which interacts with the extended Tyr–Cys system (Whittaker *et al.*, 1993). In the case of human cysteine dioxygenase the Tyr–Cys cofactor enables the Tyr hydroxyl group to stabilize the oxygen radical formed during catalysis, thus preventing the formation of damaging hydroxyl radicals (Ye *et al.*, 2007). No structural/functional implications for the Tyr–Cys bond in *M. tuberculosis* nitrite reductase have been suggested which could explain the reduced activity of the mutant forms of this enzyme without the Tyr–Cys bond (Cys was replaced; Schnell *et al.*, 2005).

In several TvNiR structures we found an unusual covalent bond between the side chains of the catalytic tyrosine residue and the glutamine involved in coordination of the calcium ion, the appearance of this bond being unclear. The modified form of the enzyme (referred to in the following as TvNiRb) was then obtained deliberately by cocrystallization of TvNiR with hydroxylamine. The presence of the Tyr–Gln bond in TvNiRb was reliably confirmed in the structure determined at 1.45 Å resolution. The activities of TvNiR and TvNiRb are quantitatively characterized and the influence of the Tyr–Cys and Tyr–Gln bonds on the activity of cytochrome *c* nitrite reductase is considered. The structures of TvNiRb in complex with sulfite and of TvNiR in complex with nitrite were determined, with both structures being characterized by full occupancy of the substrate site.

Table 2
Data-collection and structure-refinement statistics.

Values in parentheses are for the last resolution shell.

	TvNiR–NO_2	TvNiRb–PO_4	TvNiRb–SO_3	TvNiRb–SO_3(MV)	TvNiRb–NH_2OH	TvNiRb–H_2O
PDB code	3rkh	3sce	3lgq	3lg1	3s7w	3uu9
X-ray source	K4.4	SPring-8 BL41XU	DESY X13	K4.4	DESY X13	K4.4
Wavelength (Å)	0.978	0.750	0.812	0.989	0.812	0.978
Resolution (Å)	1.83 (1.90–1.83)	1.45 (1.60–1.45)	1.80 (1.85–1.80)	1.95 (2.00–1.95)	1.79 (1.85–1.79)	2.20 (2.50–2.20)
Unit-cell parameter (Å)	192.80	193.01	195.69	192.62	194.89	191.39
No. of measured reflections	2710187 (224205)	3195990 (553891)	666945 (34628)	1273148 (91919)	707572 (54210)	512633 (160640)
No. of unique reflections	208153 (22013)	464187 (106316)	221170 (13090)	171512 (12445)	116387 (9486)	117676 (37149)
Completeness (%)	99.8 (99.9)	99.9 (99.9)	96.6 (73.1)	99.7 (99.9)	97.2 (84.7)	99.8 (99.7)
R_{meas}†	0.120 (0.671)	0.110 (0.544)	0.066 (0.390)	0.144 (0.787)	0.071 (0.449)	0.159 (0.704)
$\langle I/\sigma(I)\rangle$	20.0 (3.9)	11.1 (3.4)	15.1 (3.1)	12.4 (2.9)	12.6 (2.7)	9.9 (2.8)
B factor from Wilson plot (Å^2)	26.2	23.8	28.0	29.2	30.6	37.0
R‡	0.141	0.124	0.151	0.161	0.153	0.157
R_{free}§	0.162	0.140	0.168	0.183	0.173	0.184
Root-mean-square deviations						
Bond lengths (Å)	0.020	0.017	0.018	0.018	0.019	0.017
Bond angles (°)	1.700	1.460	1.470	1.540	1.459	1.596
DPI (Å)	0.068	0.034	0.065	0.087	0.069	0.131
No. of protein atoms	8334	8378	8356	8287	8341	8304
No. of water molecules	1327	1186	1140	974	1088	900
Average *B* factor (Å^2)						
All atoms	16.6	16.1	25.2	21.0	27.5	35.6
Water molecules	29.9	26.0	34.0	28.7	34.8	41.6
Ligand	NO_2^-	$H_2PO_4^-$/HPO_4^{2-}	HSO_3^-	HSO_3^-	NH_2OH	H_2O/OH^-
Ligand occupancy	1	1/2	1	1/2	1/2	1
Ligand average *B* factor (Å^2)	16.9	9.3	25.1	15.0	24.0	30.2

† $R_{meas} = \sum_{hkl}\{N(hkl)/[N(hkl)-1]\}^{1/2}\sum_i |I_i(hkl) - \langle I(hkl)\rangle|/\sum_{hkl}\sum_i I_i(hkl)$, where $N(hkl)$ is the total number of times a given reflection is measured. ‡ $R = \sum_{hkl} ||F_{obs}| - |F_{calc}||/\sum_{hkl}|F_{obs}|$, where *hkl* identifies reflections included in the refinement and $|F_{obs}|$ and $|F_{calc}|$ are the observed and calculated amplitudes of the structure factors, respectively. § $R_{free} = \sum_{hkl} ||F_{obs}| - |F_{calc}||/\sum_{hkl}|F_{obs}|$, where *hkl* identifies reflections that were not included in the refinement.

2. Materials and methods

2.1. Preparation of TvNiR and TvNiRb complexes

TvNiR was purified as described previously (Filimonenkov *et al.*, 2010; Tikhonova *et al.*, 2010). The modified form TvNiRb was obtained by chance in one of the isolations, which involved an additional step of precipitation of the protein with ammonium sulfate. The reasons for the appearance of this modification remain unclear; however, it is unlikely that ammonium sulfate by itself can lead to formation of the Tyr–Gln bond.

Crystals of TvNiR and the modified form TvNiRb were grown by the hanging-drop vapour-diffusion method under conditions similar to those described previously (Boyko *et al.*, 2006). Drops consisted of equal volumes of protein solution and reservoir solution. The conditions for preparation of the TvNiR and TvNiRb complexes by cocrystallization are given in Table 1. The reservoir solutions used for preparation of the TvNiR–NO_2, TvNiRb–SO_3 and TvNiRb–NH_2OH complexes contained the component necessary for the formation of a particular complex at 0.1 *M*. Crystals of TvNiRb in complex with phosphate were obtained using protein solution containing potassium phosphate buffer. Crystals of the TvNiRb–H_2O complex were prepared by cocrystallization of non-modified TvNiR with hydroxylamine.

The TvNiRb–SO_3(MV) complex was obtained by soaking a crystal of the phosphate complex of TvNiRb in reservoir solution containing 0.08 *M* Na_2SO_3, 0.13 *M* $NaBH_4$ and 0.02 *M* methyl viologen (MV) for 10 min. Sodium borohydride was used for reduction of the haems. The reduction of TvNiR by sodium borohydride in solution was confirmed by the characteristic peaks of the haems in the absorption spectrum of the protein (at 525 and 554 nm). In the case of the preparation of the TvNiRb–SO_3(MV) complex, the presence of the reducing medium during the soaking process was indicated by the blue colour of the solution (which arises from the presence of reduced methyl viologen).

2.2. X-ray diffraction data collection and processing and structure refinement

X-ray diffraction data were collected on the K4.4 beamline at the RRC 'Kurchatov Institute' (Russia), on the X13 beamline at DESY (Germany) and on the BL41XU beamline at SPring-8 (Japan) at 100 K. X-ray data-collection statistics are given in Table 2.

The X-ray diffraction data were processed using the *XDS* and *XSCALE* programs (Kabsch, 2010). The crystals of TvNiR and TvNiRb belonged to space group $P2_13$. The structure of free TvNiR (PDB entry 2ot4; Polyakov *et al.*, 2009) was used as a starting model for the refinement of the structures of the complexes. Refinement was performed using the *REFMAC*5 program (Murshudov *et al.*, 2011). The structure of the TvNiRb–PO_4 complex was refined anisotropically. Manual corrections of the models were performed based on the analysis of difference Fourier maps using *Coot* (Emsley &

Cowtan, 2004). Organic molecules that were present in the crystallization solutions were located in the structures. The structures were analyzed using the *CCP*4 program suite (Winn *et al.*, 2011). Structure-refinement statistics are given in Table 2.

2.3. Activity measurements

The catalytic reduction of nitrite and sulfite was performed in an anaerobic glove box (Belle Technology, UK) at a residual oxygen pressure of at most 2 p.p.m. at 293 K in 0.05 *M* potassium phosphate buffer pH 7.0. Methyl viologen (MV) pre-reduced with europium(II) chloride was used as a reducing agent. 0.3 *M* MV in 0.5 *M* phosphate buffer pH 7.0 was reduced using 0.2 *M* $EuCl_2$. Upon this, Eu^{III} phosphates precipitated. The supernatant with reduced MV was used then in activity assays (2–3 µl per millilitre of the reaction mixture). The addition of this MV solution to the reaction buffer did not change the pH value of the buffer.

The nitrite reductase activities of TvNiR and TvNiRb were determined using two methods based on the rate of nitrite reduction and the rate of MV oxidation. The reaction was initiated by the addition of sodium nitrite.

In the former case, the maximum rate of the catalytic reaction was measured at an enzyme concentration of 4×10^{-4} mg ml^{-1} and an initial sodium nitrite concentration of 1 m*M*. Aliquots were taken from the reaction mixture at 30 s intervals after the beginning of the reaction. The nitrite concentration in the preparations was detected by the formation of the colored diazo compound as described in Nicolas & Nason (1957).

Measurements of the activities of TvNiR and TvNiRb from the rate of MV oxidation were performed at an enzyme concentration of 2.3×10^{-5} mg ml^{-1}. The initial sodium nitrite concentration was 91 µ*M*, which is approximately equal to the K_m of TvNiR for nitrite (Tikhonova *et al.*, 2010). The rate of MV oxidation was measured spectrophotometrically from a decrease in the absorption of the reaction mixture at λ = 601 nm (ε_{601} = 13.6 mM^{-1} cm^{-1}). Under these conditions, the rate of non-enzymatic oxidation of MV by nitrite is much lower than the rate of oxidation in the presence of the enzyme (see Supplementary Fig. 1[1]). The rate of non-enzymatic oxidation of MV by nitrite was subtracted from the total rate of MV oxidation in the experiment. The maximum rates were evaluated by multiplying the experimental rates by a factor of two.

The sulfite reductase activity of TvNiR was determined from the rate of MV oxidation measured spectrophotometrically based on the decrease in the absorption of the reaction mixture at λ = 601 nm. The reaction was initiated by the addition of sodium sulfite. The TvNiR concentration was 0.06 mg ml^{-1}. The initial sodium sulfite concentration was 4.5 m*M*.

[1] Supplementary material has been deposited in the IUCr electronic archive (Reference: DW5005). Services for accessing this material are described at the back of the journal.

3. Results

3.1. Structure of the modified form of the enzyme TvNiRb and its comparison with that of TvNiR

In the TvNiRb–PO_4, TvNiRb–SO_3, TvNiRb–SO_3(MV) and TvNiRb–NH_2OH complex structures we found an unusual covalent bond between the CE1 atom of the catalytic Tyr303 and the CG atom of Gln360, which is involved in coordination to the calcium ion. Fig. 1 shows the electron density for Tyr303, Cys305 and Gln360 and the calcium ion in the TvNiRb–PO_4 structure (1.45 Å resolution). The Tyr–Gln covalent bond is of no doubt, as is the Tyr–Cys covalent bond, which is present in all TvNiR structures. The Tyr–Gln bond length in the TvNiRb structures is 1.52 ± 0.02 Å on average. This bond deviates from the plane of the aromatic ring by ∼19°. In contrast, the S atom of Cys305 lies in the plane of the tyrosine aromatic ring. The average length of the Tyr–Cys covalent bond in the TvNiR structures is 1.68 ± 0.02 Å.

The active site of TvNiRb is more rigid than that of TvNiR owing to the presence of the additional Tyr–Gln covalent bond (Tyr303 has almost the same side-chain conformation in all TvNiRb structures). Based on the superposition, using the atoms of haem 4 (r.m.s.d. 0.06 Å), of the TvNiRb–SO_3 structure and the TvNiR complex with sulfite (PDB entry 3fo3), the side chains of the catalytic His and Arg residues are almost ideally superimposed (the maximum deviation is 0.17 Å), whereas the side-chain conformations of the catalytic tyrosine residues are somewhat different. The tyrosine ring of Tyr303 in the TvNiRb structure is rotated about the CD2—CE2 bond by ∼12° compared with its position in TvNiR. The largest deviations are observed for the OH, CZ, CE1 and CD1 atoms of the tyrosine (0.4–0.7 Å). The conformation of Gln360 in TvNiRb substantially differs from that in TvNiR (Fig. 2).

In TvNiRb–PO_4, TvNiRb–SO_3(MV) and TvNiRb–NH_2OH, the conformation of Lys188 coordinated to haem 4 differs from that in the structures of non-modified TvNiR (Fig. 2). However, the Fe—NZ distance in these structures is equal to that in TvNiR (∼1.9 Å). There are no other structural differences between TvNiRb and TvNiR which could be associated with the covalent Tyr–Gln modification.

In the structure of the free form of TvNiR (PDB entry 2ot4), the distal coordination site of haem 4 is occupied by a water molecule. A total of six water molecules capable of forming hydrogen bonds with the coordinated ligand were located near the distal coordination site in the various structures. These molecules are shown in Fig. 2. The molecule W1 is linked to the carboxyl groups of the haem and is present in all TvNiR, TvNiRb and NrfA structures, W2 is located above the coordination site of the haem and W3, W4 and W5 are located at the entrance to the active site, with W3 and W4 interacting with the guanidine group of Arg131 and W5 being hydrogen-bonded to the Tyr303 hydroxyl group.

3.2. Binding of the nitrite ion in the active site of cytochrome *c* nitrite reductase

A nitrite ion at full occupancy was found in the active site in the TvNiR–NO_2 structure (Fig. 3). The Fe—N(NO_2^-) distance

is 1.82 Å. The O2 atom of nitrite is hydrogen-bonded to the OH atom of Tyr303, the NE2 atom of His361 and the water molecule W2. The O1 atom of nitrite forms hydrogen bonds to the NH2 atom of Arg131 and W2. On the whole, the binding of the nitrite in TvNiR–NO_2 is similar to that observed in the nitrite complex of TvNiR containing the ligand at partial occupancy determined previously (1.78 Å resolution; PDB entry 3d1i; Polyakov *et al.*, 2009).

For NrfA, two structures of complexes with nitrite have been determined: those of the wild-type enzyme (PDB entry 2e80; 1.6 Å resolution; Einsle *et al.*, 2002) and a mutant form (Y218F) of NrfA (PDB entry 3bnh; 1.75 Å resolution) in which the catalytic tyrosine residue is replaced by phenylalanine (Lukat *et al.*, 2008). In the structures of the nitrite complexes of TvNiR and NrfA and the mutant form of NrfA superimposed using the atoms of the catalytic haems (r.m.s.d. of 0.2 Å for TvNiR–NrfA) the side chains of the catalytic histidine and the guanidine groups of the catalytic arginine superimpose well on each other. The position of the nitrite ion in the TvNiR complex is similar to that in the mutant form of NrfA. The binding of the nitrite in these structures differs only in that there is a hydrogen bond between the O2 atom of the nitrite and the hydroxyl group of the catalytic tyrosine in TvNiR, whereas a hydrogen bond between the O1 atom of the nitrite and the water molecule W5 located at the entrance to the active site is observed in NrfA. In the structure of the nitrite complex of wild-type NrfA, the position of the nitrite ion is somewhat different. In the latter structure the nitrite is not hydrogen bonded to the catalytic tyrosine residue because the side-chain conformation of the tyrosine in this structure is the same as in the structure of the free form of NrfA (PDB entry 1fs7; Einsle *et al.*, 2002; the distance between the O atom of the nitrite and the OH atom of the tyrosine is 3.8 Å). In addition, the nitrite ion in the NrfA complex is characterized by a distorted geometry and substantially different atomic temperature factors, which indicates that the interpretation of the electron density for the ligand on the distal side of the haem could be ambiguous.

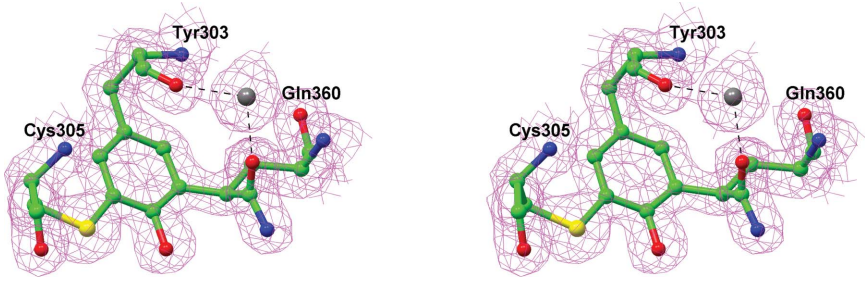

Figure 1
Stereoview of Tyr303, Cys305 and Gln360 in the active site of TvNiRb (TvNiRb–PO_4 structure at 1.45 Å resolution). The $2F_o - F_c$ electron density is contoured at the 1σ level. The calcium ion is shown as a grey sphere.

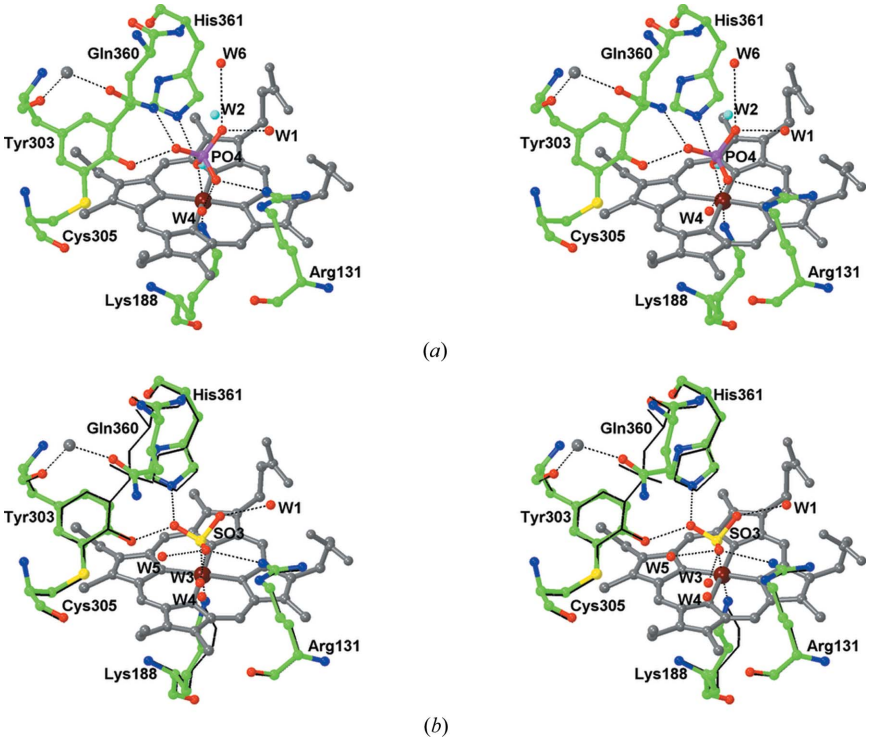

Figure 2
(*a*) Stereoview of the active site in the TvNiRb–PO_4 complex. The occupancy (z) of the phosphate site is 1/2. The water molecules (z = 1/2) that are present in the active site if the phosphate ion is absent are shown as cyan spheres. The iron ion of haem 4 is coloured brown and the protoporphyrin is coloured grey. The hydrogen and coordination bonds are represented by dashed lines. (*b*) Stereoview of the active site of TvNiR in the complex with sulfite (1.4 Å resolution; PDB entry 3fo3). The active-site residues of TvNiRb–PO_4 are represented by black lines. The structures were superimposed using the atoms of haems 4.

3.3. Structure of TvNiRb in complex with phosphate

Phosphate binds to the active site of TvNiRb in the same way as in TvNiR (PDB entry 3gm6, 1.79 Å resolution; Trofimov, Polyakov, Boiko, Filimonenkov *et al.*, 2010; Fig. 2*a*). In the TvNiRb–PO_4 structure the electron density for the distal ligand was interpreted as a phosphate ion and a water molecule with half occupancies. The second water molecule with half occupancy analogous to W2 in the free enzyme was placed near the phosphate O4 atom. It appears that the partial occupancy of the phosphate is associated with the alkaline pH value of the crystallization solution. The complex of TvNiR with phosphate (Trofimov, Polyakov, Boyko, Filimonenkov *et al.*, 2010) was obtained at a pH of ∼6.5 and

the phosphate site in the corresponding structure is fully occupied.

3.4. Structures of TvNiRb in complexes with sulfite

Two structures of TvNiRb in complex with sulfite (see §2) were determined. In the structure of the TvNiRb–SO_3 complex, which was prepared by cocrystallization of TvNiRb with sodium sulfite, the sulfite ion is present in the active site at full occupancy (Fig. 4). The S atom of the sulfite is coordinated to the haem iron ion (Fe—S, 2.26 Å) and the O atoms are hydrogen-bonded to the catalytic histidine, tyrosine and arginine residues and the water molecules W1 and W2.

The superimposition of the structures of TvNiRb–SO_3 and the complex of TvNiR with sulfite (1.4 Å resolution; PDB entry 3fo3) by the atoms of haems 4 gave a deviation of 0.55 Å for the OH atoms of Tyr303. In spite of this, the differences in the binding of the sulfite ion in the active sites of TvNiRb and TvNiR (Figs. 4 and 2*b*, respectively) are insignificant (the maximum deviation of the atoms of the sulfite ions is 0.21 Å). W3 and W5, which could be involved in hydrogen bonding to the sulfite, are absent in the TvNiRb structure, whereas W2 is absent in TvNiR. The length of the hydrogen bond between the OH atom of Tyr303 and the O2 atom of the sulfite is ∼2.66 and ∼2.55 Å in the TvNiRb and TvNiR structures, respectively.

The TvNiRb–SO_3(MV) complex was obtained from the phosphate complex of TvNiRb in the presence of the reducing agent (see §2). The electron density for the ligand on the distal side of haem 4 in this complex was interpreted as a sulfite ion and a water molecule with half occupancies. The phosphate ion was completely removed from the active site of the enzyme. The crystal structures of various TvNiR complexes with sulfite obtained from the phosphate complexes show that phosphate is replaced by sulfite with difficulty when the enzyme is in the oxidized form but is readily replaced when the enzyme is reduced (Trofimov, Polyakov, Boyko, Tikhonova *et al.*, 2010 and our unpublished data). The binding constants for sulfite are 80 µ*M* for reduced TvNiR and 1.5 m*M* for oxidized TvNiR (our unpublished data). We lack data for phosphate, but in the case of NrfA the values for another oxygen-ligating anion, nitrate, are 10 m*M* for the reduced enzyme and 73 µ*M* for the oxidized form (Gwyer *et al.*, 2006), which is in agreement with our structural data. Based on the absence of the phosphate ion in the active site of the TvNiRb–SO_3(MV) complex, as well as taking into account the conditions of the preparation of the complex, it can be concluded that we obtained the reduced form of TvNiRb.

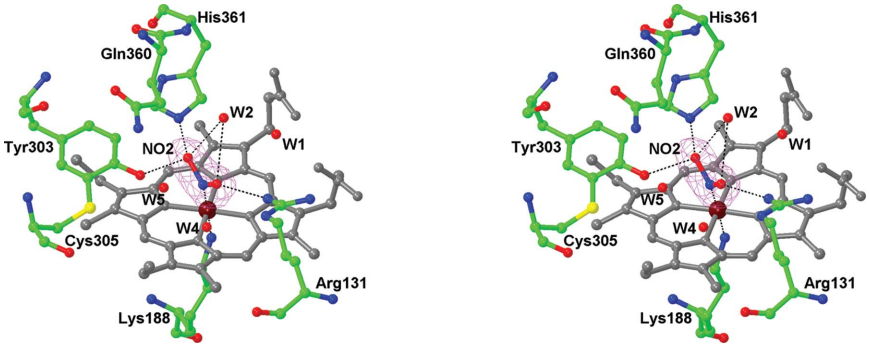

Figure 3
Stereoview of the active site in the TvNiR–NO_2 complex. The coordination and hydrogen bonds of the nitrite ion are indicated by dashed lines. The OMIT electron density (6σ) for the nitrite ion is shown. The electron-density map exactly corresponds to the $2F_o - F_c$ map in this region contoured at the 1σ level.

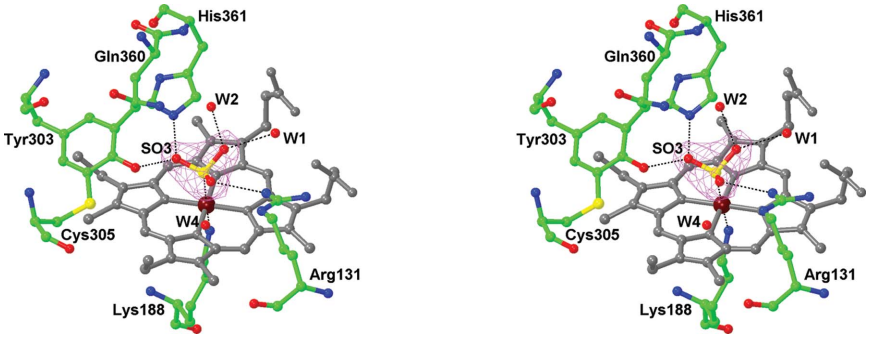

Figure 4
Stereoview of the active site in the TvNiRb–SO_3 complex. The coordination and hydrogen bonds of the sulfite ion are indicated by dashed lines. The OMIT electron density (6σ) for the sulfite ion is shown. The electron-density map exactly corresponds to the $2F_o - F_c$ map in this region countered at the 1σ level.

The binding of the sulfite ion in the TvNiRb–SO_3(MV) structure is almost the same as in TvNiRb–SO_3. In this complex the Fe—S distance is 2.23 Å; the distance between the O1 atom of the sulfite and the water molecule W1 is short (2.2–2.3 Å), with the W1 site being characterized by full occupancy. However, the partial occupancy of the sulfite site and the 1.95 Å resolution for TvNiRb–SO_3(MV) do not allow us to reliably estimate the lengths of the bonds formed by the sulfite in the active site. In the $2F_o - F_c$ electron-density map contoured at the 1σ level, the O1 atom of the sulfite and the water molecule W1 are linked by electron density. Apparently, the O1 atom of the sulfite is eliminated in the first step of reduction, resulting in the formation of an intermediate bound in the same fashion as the nitrite in the corresponding complex.

The binding of the sulfite ion in NrfA (Lukat *et al.*, 2008; Kemp *et al.*, 2010) is similar to that observed in TvNiR. In the structure of the sulfite complex of NrfA (PDB entry 3bnf), the side chain of the catalytic tyrosine residue is located closer to the distal coordination site of the catalytic haem compared with the structure of free NrfA and is hydrogen-bonded to the sulfite. The OH

Table 3
Activities of TvNiR, TvNiRb, NrfA and SiR.

The activities for NrfA and SiR were converted to s^{-1}.

Enzyme	k_{cat} (s^{-1})	
	NO_2^-	HSO_3^-
TvNiR	2860	0.039
TvNiRb	1195	0.023
NrfA (*S. deleyianum*; Schumacher *et al.*, 1994; Stach *et al.*, 2000)	960	0.336
NrfA (*W. succinogenes*; Lukat *et al.*, 2008)	380	0.122
SiR (*D. desulfuricans*; Steuber *et al.*, 1995)		0.028

atoms of the catalytic tyrosine residue in the structures of the sulfite complexes of TvNiR and NrfA superimposed using the atoms of the catalytic haems (r.m.s.d. 0.18 Å) are in close proximity (0.4 Å). In both structures the length of the hydrogen bond between the O2 atom of the sulfite and the OH atom of the tyrosine is ∼2.6 Å.

3.5. Structures of TvNiRb–NH_2OH and TvNiRb–H_2O

Hydroxylamine is itself a substrate and a possible intermediate in the reduction of nitrite to ammonia catalyzed by cytochrome *c* nitrite reductase (Einsle *et al.*, 2002; Stach *et al.*, 2000). In the TvNiRb–NH_2OH structure the electron density for the ligand on the distal side of the haem was interpreted as a hydroxylamine molecule inclined toward Arg131 and a water molecule with half occupancies (Fig. 5). In the structure of NrfA in complex with hydroxylamine (PDB entry 2e81; Einsle *et al.*, 2002), the NH_2OH molecule is located in a similar way.

In the course of structure refinement of TvNiRb–NH_2OH, a strong peak was located in the electron-density map near the CG atom of Gln360 (Fig. 5). This peak was interpreted as an O atom (of a hydroxyl group) with half occupancy covalently bound to the CG atom of glutamine (the CG—OH bond length is 1.43 Å). The O atom of NH_2OH is at hydrogen-bonding distances from the hydroxyl group of Gln360 and W3. W2 has half occupancy and is present in the structure if the distal coordination site is occupied by a water molecule.

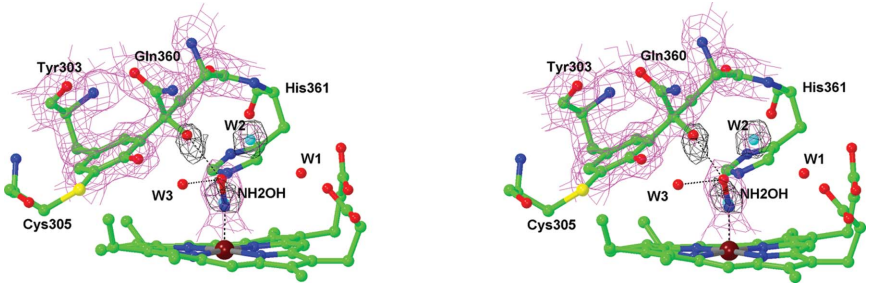

Figure 5
Stereoview of the active site in the TvNiRb–NH_2OH complex from the side of Arg131. The occupancy (z) of the hydroxylamine site is 1/2. The water molecules that are present in the active site in the absence of hydroxylamine are represented as cyan spheres. The coordination and hydrogen bonds of the hydroxylamine molecule are indicated by dashed lines. The $F_o - F_c$ (black, 6σ) and $2F_o - F_c$ (violet, 1.5σ) maps are shown. The OH group at the CG atom of Gln360 (z = 1/2), the water molecule coordinated to the haem Fe atom (z = 1/2) and the water molecule W2 (z = 1/2) were excluded from the phase calculations.

The modified form TvNiRb was obtained by cocrystallization of the free form of nonmodified TvNiR with hydroxylamine (the TvNiRb–H_2O structure). Despite the fact that the TvNiRb–H_2O structure was determined at relatively low resolution (2.2 Å), the electron density for the Tyr–Gln covalent bond is beyond doubt. The electron density for the distal coordination site can be described by a water molecule with full occupancy. The side-chain conformations of His361 and Arg131 and the arrangement of the water molecules in the active site of TvNiRb–H_2O are the same as those observed in the structure of the free form of nonmodified TvNiR.

In our opinion, the formation of the Tyr–Gln covalent bond occurs by a radical mechanism. It is known that hydroxylamine is slowly oxidized in solution by molecular oxygen in the presence of traces of transition metals to form a nitrite ion, a superoxide radical and hydrogen peroxide (Kono, 1978). The subsequent reaction of hydrogen peroxide with the iron ion of the catalytic haem (the peroxidase activity of TvNiR has been revealed previously; Tikhonova *et al.*, 2006) in the presence of oxygen can lead to oxidation of nearby amino-acid residues, with Tyr303 being the most sensitive. The resulting tyrosyl radical, which is stabilized owing to electron delocalization over the *ortho* and *para* positions of the phenyl ring, reacts with the nearby CG atom of Gln360 (at a distance of 3.7 Å) to form a covalent bond characteristic of TvNiRb. In TvNiRb the CG atom of Gln360 tends to oxidize further owing to the influence of the phenyl ring of Tyr303 and the amide group coordinated to the calcium ion, which create a partial positive charge at CG. This is why the cocrystallization of TvNiRb with hydroxylamine resulted in hydroxylation of the CG atom of Gln360 (Fig. 5). It should be noted that in all structures of NrfA from *Wolinella succinogenes* partial *ortho*-hydroxylation of Tyr219, which is close to the active site, was observed (Einsle *et al.*, 2000).

3.6. Catalytic activity of TvNiR and TvNiRb

Table 3 gives the activities of TvNiR, TvNiRb, NrfA and SiR. The nitrite reductase activity of TvNiR measured under anaerobic conditions at pH 7.0 and 293 K and calculated from the oxidation rate of reduced MV was 2860 ± 290 NO_2^- s^{-1}. This value is close to that evaluated previously from the rate of consumption of nitrite with the use of sodium dithionite for the reduction of MV and the protein (2220 NO_2^- s^{-1}; Tikhonova *et al.*, 2010); however, the previously used method is less reliable because of inhibition of the nitrite reductase activity by sulfite that is formed upon oxidation of dithionite.

The nitrite reductase activity of TvNiRb, which was calculated from the oxidation rate of reduced MV measured under the same conditions as the activity of nonmodified TvNiR, is 1195 ± 95 NO_2^- s^{-1}. This value is similar to

the nitrite reductase activity of NrfA from *Sulfurospirillum deleyianum* (960 NO_2^- s^{-1}, which is the highest published nitrite reductase activity for NrfA; Stach *et al.*, 2000). Supplementary Fig. 1 shows a plot of the oxidation rate of MV *versus* the TvNiRb concentration. The activity of TvNiRb at pH 7.0 and 293 K measured from the rate of consumption of nitrite is 910 ± 220 NO_2^- s^{-1}, which is equal within experimental error to the value given above.

The sulfite reductase activity of TvNiR at pH 7.0 and 293 K evaluated from the oxidation rate of reduced MV is 0.039 ± 0.007 HSO_3^- s^{-1}, which is 1.7 times higher than the activity of TvNiRb determined previously under the same conditions (Trofimov, Polyakov, Boyko, Tikhonova *et al.*, 2010). It should be noted that in this study (Trofimov, Polyakov, Boyko, Tikhonova *et al.*, 2010) the sulfite reductase activity of TvNiR was measured using a TvNiRb preparation (this fact was revealed in subsequent structural studies) and the activities reported in the study refer not to TvNiR (as has been stated) but to TvNiRb. The sulfite reductase activity of TvNiR is 3.1 times lower than that of NrfA from *W. succinogenes* (the lowest published activity for NrfA; Lukat *et al.*, 2008) but is comparable with the activity of sirohaem-containing sulfite reductase from *Desulfovibrio desulfuricans* (Steuber *et al.*, 1995).

3.7. Putative proton-transport channel in TvNiR

The TvNiR structure has a channel through which protons from the surface of the protein can be transferred to W5 and the hydroxyl group of Tyr303 (Fig. 6). This channel contains a chain of five water molecules. W7 is hydrogen bonded to W5 at the entrance to the active site and is linked to the NE2 and OD1 atoms of Gln360 and Asn306 of the channel, respectively. W8 is linked to the calcium ion and is located at hydrogen-bonding distances from the NE2 and OE1 atoms of Gln360, the OD1 atom of Asn306, the OD2 atom of Asp346 and W9. W9 forms a coordination bond to the calcium ion and hydrogen bonds to the OE2 atom of Glu302, the OD1 atom of Asp346 and the OD1 atom of Asn304. W10 is hydrogen bonded to the OD1 atom of Asp346, the OH atom of Tyr335 and W11 at the surface of the protein. W11 forms hydrogen bonds to the OH atom of Tyr473 and the O atom of Phe344. The width of this channel excludes the possibility of the transport of substrate and product ions along the channel.

In the NrfA structures this channel is closed at the surface of the protein by the arginine side chain and within the channel by tyrosine and leucine (or isoleucine) side chains, the positions of which in the TvNiR structure are occupied by Tyr473, Ala339 and Pro357, respectively (Fig. 6).

4. Discussion

In the structure of the nitrite complex of NrfA, the nitrite ion is hydrogen-bonded to the catalytic histidine and arginine residues, owing to which the role of the tyrosine in the active site of NrfA has escaped attention for a long time. It is believed that the histidine and arginine residues facilitate the heterolysis of the N—O bond of nitrite by creating asymmetry in the two N—O bonds (one bond is double and the other bond is single). The histidine serves as a proton donor and is present in the doubly protonated imidazolium form (Einsle *et al.*, 2002). The replacement of the tyrosine in the active site of NrfA by Phe led to a decrease in the nitrite reductase activity by two orders of magnitude, which is indicative of direct involvement of the tyrosine in the catalysis. The important role of the tyrosine is additionally confirmed by the structure of NrfA in complex with another substrate, sulfite, in which there is a hydrogen bond between the tyrosine residue and the substrate (Lukat *et al.*, 2008). Nevertheless, the role of the catalytic tyrosine in NrfA remains unclear.

In TvNiR, the Tyr–Cys covalent bond causes the side chain of the catalytic tyrosine to move closer to the distal coordination site of the haem compared with NrfA. As a result, the binding of

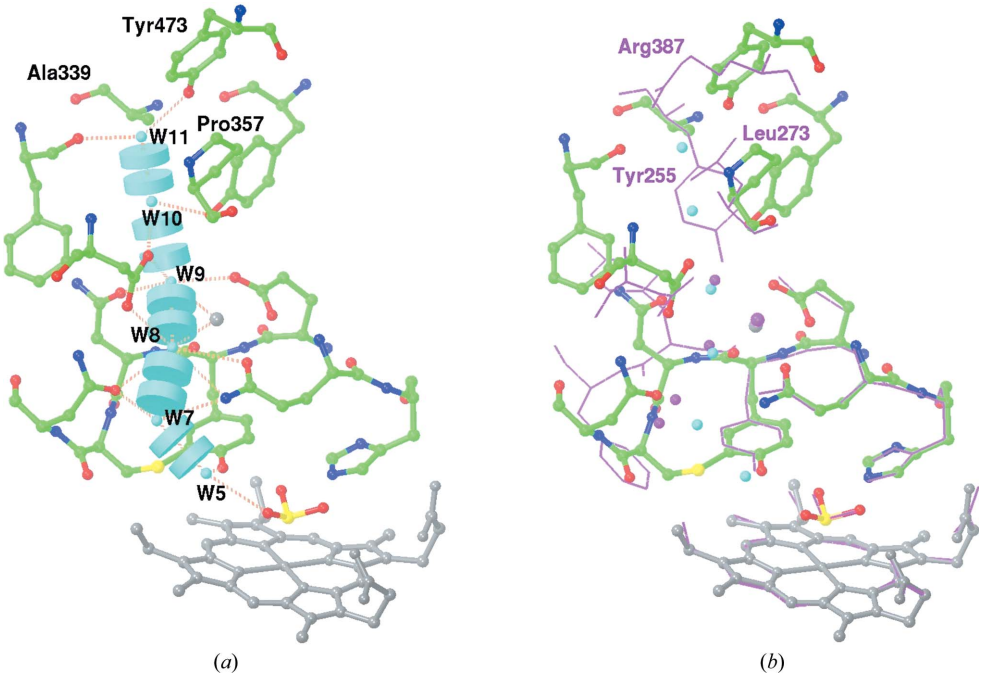

Figure 6
(*a*) The proton-transport channel in the structure of TvNiR in complex with sulfite. The channel is represented as cyan cylinders. Haem 4 and the calcium ion are shown in grey. The dashed lines indicate short contacts corresponding to hydrogen and coordination (with the calcium ion) bonds formed by the water molecules in the channel. (*b*) Superimposition of the structures of the sulfite complexes of TvNiR and NrfA from *W. succinogenes* (violet) by the atoms of the catalytic haems. The residues that block the channel in NrfA are labelled.

nitrite and sulfite in the enzyme active site is accompanied by hydrogen bonding to the catalytic Tyr303 (Polyakov *et al.*, 2009; Trofimov, Polyakov, Boyko, Tikhonova *et al.*, 2010) and the latter can act as a direct proton donor in the course of catalysis, along with His361. In this case, modifications of the tyrosine accompanied by a change in its position and the pK_a value should influence the catalytic activity of the enzyme. According to the results of quantum-chemical calculations for *o*-(methylthio)phenol in aqueous solution, the methylthio group (–SCH_3) in the *ortho* position of phenol decreases the pK_a of the hydroxyl group by 0.5 units (Himo *et al.*, 2002). Therefore, the formation of the Tyr–Cys covalent bond makes the hydroxyl group of Tyr303 a more efficient proton donor. This appears to be one of the factors that are responsible for the nitrite reductase activity of TvNiR being almost three times higher than that of NrfA (Table 3).

TvNiRb, in which the catalytic tyrosine residue forms an additional Tyr–Gln covalent bond, may be useful in investigating the role of Tyr303 in catalysis by TvNiR. A comparison of the structures of TvNiR and TvNiRb in complexes with sulfite and phosphate showed that the ligands are bound in the same fashion in the active sites of both forms. This fact, as well as the fact that binding of the ligands in TvNiRb does not lead to changes in the positions of the active-site residues, suggests that the binding of the nitrite in TvNiRb is the same as in TvNiR. Hence, a decrease in the nitrite reductase activity of TvNiRb by a factor of 2.4 compared with TvNiR may be attributed to a change in the pK_a value of Tyr303 owing to formation of the Tyr–Gln bond. The positive inductive effect of the covalently bound glutamine in the *ortho* position with respect to the tyrosine hydroxyl group should partially compensate for the influence of the covalently bound cysteine in another *ortho* position, resulting in an increase in the pK_a of the tyrosine hydroxyl group.

The arrangement and the binding of sulfite are almost identical in the active sites of TvNiR, TvNiRb, NrfA and the Y218F mutant form of NrfA (Lukat *et al.*, 2008). A decrease in the sulfite reductase activity of TvNiRb by a factor of 1.7 compared with TvNiR can also be accounted for by an increase in the pK_a of the tyrosine. In this case, the effect is smaller than that in the nitrite reduction. It appears that fast proton transfer from the hydroxyl group of the tyrosine to the substrate is less important for efficient catalysis in the case of the relatively slow sulfite-reduction reaction compared with the fast nitrite reduction, and the water molecule W5 at the entrance to the active site can serve as the proton donor instead of the tyrosine residue. For NrfA the sulfite reductase activity of the wild-type enzyme is equal within experimental error to that of the Y218F mutant form (Lukat *et al.*, 2008), which is evidence in support of the latter hypothesis.

Nitrite and sulfite reduction by cytochrome *c* nitrite reductase is accompanied by the transfer of eight or six protons, respectively. In the case of TvNiR, proton transport to the active site may occur not only through the substrate- and product-transport channels, which are similar in TvNiR and NrfA, but also through the additional proton-transport channel. The presence of the latter channel in TvNiR may be one of the factors that are responsible for the higher nitrite reductase activity of TvNiR compared with NrfA. The arrangement of Tyr303 at the exit from the proton-transport channel is evidence in favour of the involvement of this residue as the proton donor in the catalysis, which accounts for the high sensitivity of the activity of TvNiR to modification of this residue.

5. Conclusions

It is notable that the Tyr–Cys bond appears in all TvNiR structures and is suggested to occur in the native form of TvNiR in cells, whereas the Tyr–Gln bond firstly appeared as an artifact resulting from the protein-purification stage. However, it cannot be ruled out that the Tyr–Gln bond may also be formed in cells and plays a certain regulatory role. The changes in the pK_a value of the catalytic Tyr residue upon the formation of Tyr–Cys and Tyr–Gln bonds are relatively small but appear to be sufficient to influence the catalytic properties of cytochrome *c* nitrite reductase. Based on the structure of the nitrite complex of TvNiR with full active-site occupancy by nitrite, Tyr is likely to donate its proton to the nitrite during catalysis. Without making TvNiR mutants, we managed to demonstrate the latter by comparing TvNiR with TvNiRb, both of which are characterized by compact and rigid active sites, with the only significant difference concerning the pK_a value of the catalytic Tyr residue.

This work was supported by the Federal Target Program 'Scientific and Scientific Pedagogical Personnel of the Innovative Russia in 2009–2013' (Government Contracts 14.740.11.0632 and P1197) and the Russian Foundation for Basic Research (grants 10-04-01695 and 11-04-01613).

References

Bamford, V. A., Angove, H. C., Seward, H. E., Thomson, A. J., Cole, J. A., Butt, J. N., Hemmings, A. M. & Richardson, D. J. (2002). *Biochemistry*, **41**, 2921–2931.

Boyko, K. M., Polyakov, K. M., Tikhonova, T. V., Slutsky, A., Antipov, A. N., Zvyagilskaya, R. A., Bourenkov, G. P., Popov, A. N., Lamzin, V. S. & Popov, V. O. (2006). *Acta Cryst.* F**62**, 215–217.

Cunha, C. A., Macieira, S., Dias, J. M., Almeida, G., Goncalves, L. L., Costa, C., Lampreia, J., Huber, R., Moura, J. J., Moura, I. & Romão, M. J. (2003). *J. Biol. Chem.* **278**, 17455–17465.

Einsle, O., Messerschmidt, A., Huber, R., Kroneck, P. M. & Neese, F. (2002). *J. Am. Chem. Soc.* **124**, 11737–11745.

Einsle, O., Messerschmidt, A., Stach, P., Bourenkov, G. P., Bartunik, H. D., Huber, R. & Kroneck, P. M. (1999). *Nature (London)*, **400**, 476–480.

Einsle, O., Stach, P., Messerschmidt, A., Simon, J., Kröger, A., Huber, R. & Kroneck, P. M. (2000). *J. Biol. Chem.* **275**, 39608–39616.

Emsley, P. & Cowtan, K. (2004). *Acta Cryst.* D**60**, 2126–2132.

Filimonenkov, A. A., Zvyagilskaya, R. A., Tikhonova, T. V. & Popov, V. O. (2010). *Biochemistry*, **75**, 744–751.

Gwyer, J. D., Richardson, D. J. & Butt, J. N. (2006). *Biochem. Soc. Trans.* **34**, 133–135.

Himo, F., Noodleman, L., Blomberg, M. R. A. & Siegbahn, P. E. M. (2002). *J. Phys. Chem.* **106**, 8757–8761.

Ito, N., Phillips, S. E., Stevens, C., Ogel, Z. B., McPherson, M. J., Keen, J. N., Yadav, K. D. & Knowles, P. F. (1991). *Nature (London)*, **350**, 87–90.
Joseph, C. A. & Maroney, M. J. (2007). *Chem. Commun.*, pp. 3338–3349.
Kabsch, W. (2010). *Acta Cryst.* D**66**, 125–132.
Kemp, G. L., Clarke, T. A., Marritt, S. J., Lockwood, C., Poock, S. R., Hemmings, A. M., Richardson, D. J., Cheesman, M. R. & Butt, J. N. (2010). *Biochem. J.* **431**, 73–80.
Kern, M. & Simon, J. (2009). *Biochim. Biophys. Acta*, **1787**, 646–656.
Kono, Y. (1978). *Arch. Biochem. Biophys.* **186**, 189–195.
Lukat, P., Rudolf, M., Stach, P., Messerschmidt, A., Kroneck, P. M., Simon, J. & Einsle, O. (2008). *Biochemistry*, **47**, 2080–2086.
Murshudov, G. N., Skubák, P., Lebedev, A. A., Pannu, N. S., Steiner, R. A., Nicholls, R. A., Winn, M. D., Long, F. & Vagin, A. A. (2011). *Acta Cryst.* D**67**, 355–367.
Nicolas, D. J. D. & Nason, A. (1957). *Methods Enzymol.* **3**, 981–984.
Polyakov, K. M., Boyko, K. M., Tikhonova, T. V., Slutsky, A., Antipov, A. N., Zvyagilskaya, R. A., Popov, A. N., Bourenkov, G. P., Lamzin, V. S. & Popov, V. O. (2009). *J. Mol. Biol.* **389**, 846–862.
Richardson, D. J. & Watmough, N. J. (1999). *Curr. Opin. Chem. Biol.* **3**, 207–219.
Rodrigues, M. L., Oliveira, T. F., Pereira, I. A. & Archer, M. (2006). *EMBO J.* **25**, 5951–5960.
Schnell, R., Sandalova, T., Hellman, U., Lindqvist, Y. & Schneider, G. (2005). *J. Biol. Chem.* **280**, 27319–27328.
Schumacher, W., Hole, U. & Kroneck, P. M. (1994). *Biochem. Biophys. Res. Commun.* **205**, 911–916.
Simon, J. (2002). *FEMS Microbiol. Rev.* **26**, 285–309.
Sorokin, D. Y., Antipov, A. N. & Kuenen, J. G. (2003). *Arch. Microbiol.* **180**, 127–133.
Stach, P., Einsle, O., Schumacher, W., Kurun, E. & Kroneck, P. M. (2000). *J. Inorg. Biochem.* **79**, 381–385.
Steuber, J., Arendsen, A. F., Hagen, W. R. & Kroneck, P. M. (1995). *Eur. J. Biochem.* **233**, 873–879.
Tikhonova, T. V., Polyakov, K. M., Boyko, K. M., Safonova, T. N. & Popov, V. O. (2010). In *Handbook of Metalloproteins*, http://dx.doi.org/10.1002/0470028637.met276. New York: John Wiley & Sons.
Tikhonova, T. V., Slutsky, A., Antipov, A. N., Boyko, K. M., Polyakov, K. M., Sorokin, D. Y., Zvyagilskaya, R. A. & Popov, V. O. (2006). *Biochim. Biophys. Acta*, **1764**, 715–723.
Trofimov, A. A., Polyakov, K. M., Boyko, K. M., Filimonenkov, A. A., Dorovatovskii, P. V., Tikhonova, T. V., Popov, V. O. & Kovalchuk, M. V. (2010). *Crystallogr. Rep.* **55**, 58–64.
Trofimov, A. A., Polyakov, K. M., Boyko, K. M., Tikhonova, T. V., Safonova, T. N., Tikhonov, A. V., Popov, A. N. & Popov, V. O. (2010). *Acta Cryst.* D**66**, 1043–1047.
Whittaker, M. M., Chuang, Y. Y. & Whittaker, J. W. (1993). *J. Am. Chem. Soc.* **115**, 10029–10035.
Winn, M. D. *et al.* (2011). *Acta Cryst.* D**67**, 235–242.
Ye, S., Wu, X., Wei, L., Tang, D., Sun, P., Bartlam, M. & Rao, Z. (2007). *J. Biol. Chem.* **282**, 3391–3402.